PHYSICS OF PLASMAS **21**, 073503 (2014)

A unified analysis of plasma-sheath transition in the Tonks–Langmuir model with warm ion source

D. D. Tskhakaya, Sr.,[1,a)] L. Kos,[2] and N. Jelić[3]
[1]*Fusion@ÖAW, Institute for Theoretical Physics, University of Innsbruck, A-6020 Innsbruck, Austria*
[2]*LECAD Laboratory, Faculty of Mechanical Engineering, University of Ljubljana, SI-1000 Ljubljana, Slovenia*
[3]*Fusion@ÖAW, Institute for Theoretical and Computational Physics, TU Graz, A-8010 Graz, Austria*

(Received 27 February 2014; accepted 14 June 2014; published online 7 July 2014)

The paper presents a comprehensive kinetic theory of the famous Tonks–Langmuir model of a plane symmetric discharge, taking into account the thermal motion of ion source particles. The ion kinetics is governed by the ionization of neutrals at electron impacts. The plasma consisting of Boltzmann distributed electrons and singly charged ions is in contact with the absorbing negative wall. The derivations are performed in the frame of the "asymptotic two-scale" approximation, when the ionization mean-free path L_i is much larger than the electron Debye length λ_D. In the limit $(\lambda_D/L_i) \to 0$, the plasma-wall transition (PWT) layer can be split into two sublayers: a quasineutral presheath (PS) (with the scale-length L_i) and the Debye sheath (DS) (with the scale λ_D). Such a subdivision of the PWT layer allows to investigate these sublayers separately and simplify the analysis of the influence of the ion source thermal motion (this has been neglected in the major part of publications up to now). The uniform description of the PWT layer as a single unit is complicated by the singular presheath and sheath structure and by a coupling with the eigenvalue problem originating from the plasma balance in the bounded system. The issue is clarified both analytically and numerically by construction of a matched asymptotic expressions. The equation and the length-scale governing the transition between neighboring PS and DS sublayers are derived. The eigenvalue problem combining the wall potential, the wall location, and the ionization mean-free path is discussed. © *2014 AIP Publishing LLC*.
[http://dx.doi.org/10.1063/1.4885638]

I. INTRODUCTION

The Tonks–Langmuir (T&L) model[1] of the plane symmetric discharge is a "touchstone" for the plasma physics community, engaging the plasma-wall transition (PWT) problem. The possibility to obtain clear and transparent analytic results makes this model a very suitable bridgehead to provide new approaches and generalizations. The T&L model implies a weakly ionized one-dimensional plasma discharge confined by two parallel absorbing walls. The electrons are assumed to be Boltzmann distributed and ions are provided by electron impact ionization of neutrals. Due to mathematical difficulties and the non-triviality of the physical interpretation of results in the PWT theory, usually two main approximations are used: (i) The concept of the asymptotic two-scale (A2S) approximation[2] and (ii) the thermal motion of ion source particles is neglected, assuming the temperature of the ion source to be small.

The concept of the A2S approximation refers to the smallness of the electron Debye length λ_D in comparison with the smallest mean-free paths ℓ from the collision processes considered in the given discharge model. In the T&L model, this is the ionization mean-free path L_i, $\ell = L_i$. In the limit $\lambda_D/\ell \to 0$, the PWT layer can be split into two sublayers: the presheath (PS) (with the characteristic scale-length ℓ) and the Debye sheath (DS) (with the characteristic scale-length λ_D), which allows to investigate these sublayers separately from each other. The thin Debye sheath with its prevailing positive charge shields the quasineutral presheath from the wall, charged negatively. The presheath–sheath interface is distinguished by the electric field singularity,[3,4] indicating the breakdown of the quasineutrality condition at the presheath edge and the fulfillment of the Bohm criterion[5] in the marginal form. The electric field singularity from the presheath side indicates that in the frame of the A2S limit the subsequent interface is infinitely thin on the presheath x/ℓ-scale (x is the coordinate), while from the sheath side (i.e., on the sheath scale x/λ_D) the sheath edge is shifted into the infinity, where the electric field is zero.[6,7] Obviously, the presheath and the sheath cannot be matched smoothly without accounting for the transition region on an intermediate scale.[4,7] The intermediate scale refers exclusively to the transition region, where on the one hand, the quasineutrality condition to be violated and, on the other hand, ionization begins to become important. In other words, in the transition region both, the space charge and the ionization give small but finite contributions of the same order.

We start solving the kinetic problem from the plasma center and proceed to the wall. We use the definitions of the ion distributions function in the Debye sheath the condition at the presheath–sheath interface as a boundary condition. This procedure convenient for the PWT layer description is intrinsically connected with an eigenvalue problem—the

[a)]Also at Institute of Physics, Georgian Academy of Sciences, 0177 Tbilisi, Georgia.

 © 2014 AIP Publishing LLC

This article is copyrighted as indicated in the article. Reuse of AIP content is subject to the terms at: http://scitation.aip.org/termsconditions. Downloaded to IP: 130.183.200.242 On: Tue, 12 Aug 2014 14:08:40

wall position is not a priori given, but is an eigenvalue of the problem. This reflects the fact that the ion production rate must be equal to the rate of ions lost at the wall ("plasma balance").[4] Moving towards the wall the eigenvalue problem is simply solved by cutting all solutions at that position, where the wall boundary condition, $\Phi = \Phi_w$ is fulfilled (Φ is the electric potential). An analytic hydrodynamic description of the classical T&L model was realized in Ref. 7, where the ion source is also assumed to be cold. In Ref. 6 is formulated the comprehensive kinetic theory of the T&L model in the frame of the A2S limit using again the same approximation of *cold* ion source.

To present time, several papers[8–13] have been published, where the thermal motion of the neutral gas is taken into account. But, in all these papers, the characteristics of only quasineutral presheath are investigated (In citations above, to our knowledge, the complete number of papers dedicated to the problem is given).

In the present paper, the comprehensive kinetic theory of the whole PWT layer in the T&L model with hot neutrals is formulated. Using the A2S approximation, two neighboring sublayers—the PS, and the DS are separately studied. It is shown that the Bohm criterion at the PS–DS interface is valid also in the case of hot neutrals. The intermediate region is defined, which bridges the PS and he DS and provides for the smooth transition between these sublayers. The eigenvalue problem for definition of the wall position is discussed in Sec. IX.

II. THEORETICAL BACKGROUND

The general formulation of the problem of the plane-parallel symmetric discharge—shown in the schematic diagram, Fig. 1—consists of simultaneous solving of the Boltzmann kinetic equation for ion velocity distribution function (VDF) $f_i(x,v)$,

$$v\frac{\partial f_i}{\partial x} - \frac{e}{m_i}\frac{d\Phi}{dx}\frac{\partial f_i}{\partial v} = S_i(x,v)\,, \tag{1}$$

and Poisson's equation

$$-\frac{d^2\Phi}{dx^2} = \frac{e}{\varepsilon_0}(n_i - n_e). \tag{2}$$

The source term $S_i(x, v)$ on the right-hand side of Eq. (1) describes microscopic processes assumed for a particular scenario of interest, x being the Cartesian space coordinate, v

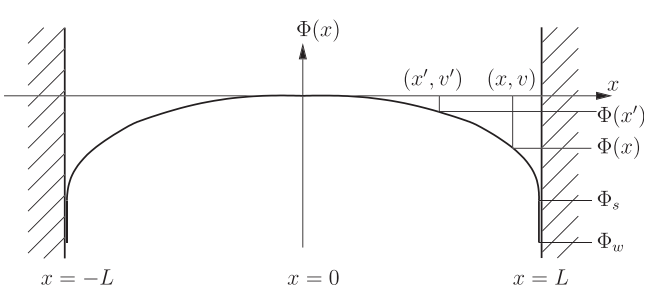

FIG. 1. The geometry and coordinate system.

the particle velocity, e the positive elementary charge, m_i the ion mass, $\Phi(x)$ the electrostatic potential at position x, ε_0 the vacuum dielectric constant, and $n_{i,e}$ are the ion and electron densities, respectively. The source term $S_i(x,v)$ can be defined in a fairly general form

$$S_i(v,x) = Rn_n n_e(x) f_n\left(\frac{v}{v_{T_n}}\right)\mathrm{H}\left(\frac{m_i v^2}{2}\right), \tag{3}$$

where R is the ionization rate, n_n is the density of ion source particles with certain velocity distribution function $f_n(v/v_{T_n})$ (which is in our case uniform over the system); the electrons follow the Boltzmann distribution. Under $n_e(x)$ in Eq. (3), further, we imply $n_e(x) = n_0 \exp(\beta e\Phi(x)/kT_e)$ with n_0 the electron density at $x = 0$. The parameter β characterizes the rate of ion generation per unit volume: when $\beta = 0$ the rate is uniform; when $\beta = 1$, the rate is proportional to the electron density. The values of β greater than unity correspond to those cases where ion generation due to ionization is a multiple stage process dependent upon the electron density;[3] $v_{T_n} = \sqrt{kT_n/m_n}$ (it is assumed that for the present investigation the neutral atom mass m_n is equal to the ion mass m_i and T_n is the ion source or, alternatively, or the ion temperature at the point of ionization. The effective ion temperature should be calculated from the final VDF of ions the neutral gas temperature.[12] $\mathrm{H}(z)$ denotes the Heaviside step function, which is introduced to comply with the positiveness of the kinetic energy of the born ion. The wall's potential is assumed to be floating. The corresponding requirement that the ion current must be equal to the electron current $\Gamma_i = \Gamma_e$ at the wall leads to writing

$$\begin{aligned}\Gamma_i &= LRn_n n_{e,av},\\ \Gamma_e &= \frac{1}{\sqrt{2\pi}} v_{T_e} n_0 \exp\left(\frac{e\Phi_w}{kT_e}\right),\end{aligned} \tag{4}$$

where $v_{T_e} = \sqrt{kT_e/m_e}$, and m_e, T_e are the electron mass and electron temperature, respectively, while Φ_w is the wall potential as indicated in Fig. 1. The expression for the ion flux in Eq. (4) can be determined from the continuity equation

$$\frac{\partial \Gamma_i}{\partial x} = Rn_n n_e(x). \tag{5}$$

In Eq. (4), $n_{e,av}$ represents average value of the electron density over the system[8]

$$n_{e,av} = \frac{1}{L}\int_0^L dx\, n_e(x).$$

The plates in Fig. 1 at $\pm L$ are assumed to be perfectly absorbing. Although the plates are grounded in an experiment, it is convenient to take the potential at the discharge center as referential, i.e., the electrostatic potential $\Phi(x)$ is assumed to be monotonically decreasing (for $x > 0$) and is defined to be zero at $x = 0$. With the help of an auxiliary function

$$F_n\left(\frac{v}{v_{T_n}}\right) = \sqrt{2\pi}\cdot v_{T_n} f_n\left(\frac{v}{v_{T_n}}\right). \tag{6}$$

This article is copyrighted as indicated in the article. Reuse of AIP content is subject to the terms at: http://scitation.aip.org/termsconditions. Downloaded to IP: 130.183.200.242 On: Tue, 12 Aug 2014 14:08:40

The source term in Eq. (3) acquires the form

$$S_i(x,v) = \frac{1}{L} B n_e(x) F_n\left(\frac{v}{v_{T_n}}\right) H\left(\frac{m_i v^2}{2}\right), \tag{7}$$

$$B = \frac{1}{2\pi}\sqrt{\frac{T_e}{T_n}\frac{m_i}{m_e}}\frac{n_0}{n_{e,av}}\exp\left(\frac{\beta e \Phi_w}{kT_e}\right). \tag{8}$$

Quantity B (originally introduced in Ref. 8) is related to the ionization frequency ν_i, and the characteristic ionization length L_i is defined as

$$\nu_i = R n_n = B\frac{\sqrt{2\pi}}{L} v_{T_n}, \quad \text{and} \quad L_i = \frac{c_s}{\nu_i} = \frac{L}{B}\sqrt{\frac{T_e}{2\pi T_n}}. \tag{9}$$

The general solution of Eq. (1) with the source term (7) is

$$f_i^{\pm}(x,v) = \bar{f}_i^{\pm}\left(v^2 + \frac{2e}{m_i}\Phi(x)\right) \pm \frac{B}{L} n_0 \times \int^x \frac{dx'}{\sqrt{v'^2}} \exp\left(\frac{\beta e \Phi(x')}{kT_e}\right) F_n\left(\pm\frac{\sqrt{v'^2}}{v_{T_n}}\right) \mathrm{H}(v'^2), \tag{10}$$

where

$$v'^2 = v^2 - \frac{2e}{m_i}\{\Phi(x') - \Phi(x)\}. \tag{11}$$

In Eq. (10), $f_i^{\pm}$ denotes the VDF of the ions moving in the positive ("+") and negative ("−") directions of the x-axis, respectively. The point (x',v') in the phase-space (see Fig. 1) is the point of the ion birth. The ion velocity at the observation point we can find from the energy conservation law (11). Further, we consider the symmetric distribution of ion source, when

$$F_n\left(+\frac{v}{v_{T_n}}\right) = F_n\left(-\frac{v}{v_{T_n}}\right). \tag{12}$$

Functions $\bar{f}_i^{\pm}(x,v)$ are arbitrary functions corresponding to the homogeneous part of Eq. (1) to be constrained by conditions as follows:

(a) at the center of the system, $x=0$, the velocity distribution function must be symmetric in the velocity space $f_i^+(0,v) = f_i^-(0,v)$, and
(b) we assume that there is a point $x_s = L_s$ ("the pre-sheath edge", see the end of Sec. IV) beyond which there are no ions with the negative velocity, $f^-(L_s, v) = 0$.

From the condition (a), we find the following connection between $\bar{f}_i^+(v^2 + 2e\Phi(x)/m_i)$ and $\bar{f}_i^-(v^2 + 2e\Phi(x)/m_i)$ arbitrary functions

$$\begin{aligned}\bar{f}_i^+(v^2 + 2e\Phi(x)/m_i) &+ \frac{B}{L} n_0 \times \int^0 \frac{dx'}{\sqrt{v'^2}} \exp\left(\frac{\beta e \Phi(x')}{kT_e}\right) F_n\left(+\frac{\sqrt{v'^2}}{v_{T_n}}\right) H(v'^2), \\ &= \bar{f}_i^-(v^2 + 2e\Phi(x)/m_i) - \frac{B}{L} n_0 \times \int^0 \frac{dx'}{\sqrt{v'^2}} \exp\left(\frac{\beta e \Phi(x')}{kT_e}\right) F_n\left(-\frac{\sqrt{v'^2}}{v_{T_n}}\right) H(v'^2),\end{aligned} \tag{13}$$

and by means of the second (b) condition, $f^-(L_s, v) = 0$, we find

$$\bar{f}_i^-(v^2 + 2e\Phi(x)/m_i) = \frac{B}{L} n_0 \times \int^{L_s} \frac{dx'}{\sqrt{v'^2}} \exp\left(\frac{\beta e \Phi(x')}{kT_e}\right) F_n\left(-\frac{\sqrt{v'^2}}{v_{T_n}}\right) H(v'^2). \tag{14}$$

Substituting Eq. (14) into (13), we obtain

$$\begin{aligned}\bar{f}_i^+(v^2 + 2e\Phi(x)/m_i) &= -\frac{B}{L} n_0 \int^0 \frac{dx'}{\sqrt{v'^2}} \exp\left(\frac{\beta e \Phi(x')}{kT_e}\right) F_n\left(+\frac{\sqrt{v'^2}}{v_{T_n}}\right) H(v'^2) \\ &+ \frac{B}{L} n_0 \int_0^{L_s} \frac{dx'}{\sqrt{v'^2}} \exp\left(\frac{\beta e \Phi(x')}{kT_e}\right) F_n\left(-\frac{\sqrt{v'^2}}{v_{T_n}}\right) H(v'^2).\end{aligned} \tag{15}$$

After straightforward calculations, we obtain the following solution of the Boltzmann kinetic equation for the arbitrary symmetric distribution function of the ion source:

$$f_i^+(x,v) = B\frac{n_0}{L}\left\{\int_0^x dx' + \int_0^{L_s} dx'\right\} F_n\left(+\frac{\sqrt{v'^2}}{v_{T_n}}\right) \times \frac{1}{\sqrt{v'^2}} \exp\left(\frac{\beta e \Phi(x')}{kT_e}\right) \mathrm{H}(v'^2), \tag{16}$$

(where brackets $\{\int\}$ denote integral operator) and

$$f_i^-(x,v) = B\frac{n_0}{L}\int_x^{L_s} dx' F_n\left(-\frac{\sqrt{v'^2}}{v_{T_n}}\right) \times \frac{1}{\sqrt{v'^2}} \exp\left(\frac{\beta e \Phi(x')}{kT_e}\right) \mathrm{H}(v'^2). \tag{17}$$

In Eqs. (16) and (17), the velocity v' is defined by expression (11). It is necessary to mention that the similar solutions are found by Riemann[14] using a different boundary condition (see the boundary condition (a) used by us above). As the definition of the ion density we have

$$n_i(x) = \int_0^{\infty} dv\{f_i^+(v,x) + f_i^-(v,x)\}. \tag{18}$$

III. MAXWELLIAN ION-SOURCE

For the Maxwellian source the auxiliary function (6) takes the form

$$F_n\left(\frac{v}{v_{T_n}}\right) = \exp\left(-\frac{v^2}{2v_{T_n}^2}\right). \tag{19}$$

In non-dimensional variables,

$$\frac{v}{\sqrt{2}c_s} \to v, \quad \frac{e\Phi(x)}{kT_e} \to \Phi(x), \quad \frac{x}{L_i} \to x, \quad \frac{n_{i,e}}{n_0} \to n_{i,e}, \quad c_s = \sqrt{\frac{kT_e}{m_i}}, \quad \frac{L_s}{L_i} \to L_s, \tag{20}$$

This article is copyrighted as indicated in the article. Reuse of AIP content is subject to the terms at: http://scitation.aip.org/termsconditions. Downloaded to IP: 130.183.200.242 On: Tue, 12 Aug 2014 14:08:40

and with the non-dimensional parameter

$$\tau \equiv \frac{T_e}{T_n} \to \frac{1}{T_n}, \tag{21}$$

the ion density for the Maxwellian ion source takes the form

$$\begin{aligned} n_i(x) = 2\bar{B}\int_0^\infty dv \int_0^{L_s} dx' \exp(\beta\Phi(x')) \\ \times \frac{\exp\{-\tau[v^2 - \Phi(x') + \Phi(x)]\}}{\sqrt{v^2 - \Phi(x') + \Phi(x)}} \\ \times H[v^2 - \Phi(x') + \Phi(x)], \end{aligned} \tag{22}$$

$$\bar{B} = \frac{L_i}{L}B. \tag{23}$$

The integral over x' in Eq. (22) can be split into two parts

$$\int_0^{L_s} dx'(\ldots) = \int_0^x dx'(\ldots) + \int_x^{L_s} dx'(\ldots). \tag{24}$$

In the first interval $(0, x)$ of the integration holds $\Phi(x') - \Phi(x) \geq 0$, and in the second $\Phi(x') - \Phi(x) \leq 0$. This allows us to use the cut-off property of the H-function, and finally, we find

$$\begin{aligned} n_i(x) = \bar{B}\int_0^1 dx' \exp[\beta\Phi(x')]\exp\left[\frac{\tau}{2}\{\Phi(x') - \Phi(x)\}\right] \\ \times \mathrm{K}_0\left(\frac{\tau}{2}|\Phi(x') - \Phi(x)|\right). \end{aligned} \tag{25}$$

In obtaining Eq. (25), the relation

$$2\int_0^\infty \frac{\exp(-\tau x^2)}{\sqrt{x^2 + a^2}} = \exp\left(\frac{\tau}{2}a^2\right)\mathrm{K}_0\left(\frac{\tau a^2}{2}\right), \tag{26}$$

with $\mathrm{K}_0(z)$—the modified Bessel function of zeroth order was employed. Equation (25) coincides with the expression for the ion density used in Refs. 8 and 9.

The expansion of $\mathrm{K}_0(z)$ for the small and large arguments are[15]

$$\mathrm{K}_0(z) = \ln\frac{2}{z\gamma_E}\left\{1 + \frac{z^2}{4}\right\} + \frac{z^2}{4} + O\left[\left(\frac{z^2}{4}\right)^2\right], \quad z \ll 1 \tag{27}$$

$$\mathrm{K}_0(z) \simeq \sqrt{\frac{\pi}{2z}}e^{-z}\left\{1 + O\left(\frac{1}{z}\right)\right\}. \quad z \gg 1 \tag{28}$$

In Eq. (27), $\gamma_E = \exp(C_E) = 1.78107$, where C_E is the Euler-Mascheroni constant. From Eq. (27), it follows that already for $z \leq 0.5$, we can neglect the high order terms and assume

$$\mathrm{K}_0(z) \simeq \ln\frac{2}{z\gamma_E}. \tag{29}$$

Really, for $z = 0.5$, the logarithmic term is $\ln z \simeq 0.65$ and $z^2/4 \simeq 0.063 \ll \ln z$.

IV. THE PRESHEATH IN THE WARM ION-SOURCE CASE

Below, we consider the case of the ion-source with high temperatures, when

$$T_n \geq |\Phi_s|. \tag{30}$$

Under this condition, which can be considered as a "warmness" condition of the ion source, we are able to realize analytic calculations whose results can be compared and confirmed by numerical ones.

For the argument of the modified Bessel function in the integrand of Eq. (25), we have the following estimation

$$\frac{|\Phi' - \Phi|}{2T_n} \leq \frac{|\Phi_s|}{2T_n}, \tag{31}$$

and according to the discussion given at the end of Sec. III [see Eq. (29)] and the condition (30) from Eq. (25) we find

$$\begin{aligned} n_i(x) = \bar{B}\int_0^1 dx' \exp[\beta\Phi(x')]\exp\left\{\frac{1}{2T_n}[\Phi(x') - \Phi(x)]\right\} \\ \times \ln\left(\frac{4T_n}{\gamma_E|\Phi(x) - \Phi(x')|}\right). \end{aligned} \tag{32}$$

In the dimensionless variables, Poisson's equation acquires the form

$$-\varepsilon^2\frac{\partial^2\Phi}{\partial x^2} = n_i - \exp[\Phi(x)], \tag{33}$$

where $\varepsilon = \lambda_D/L_s$ with the electron Debye length $\lambda_D = \sqrt{\varepsilon_0 kT_e/(e^2 n_0)}$. In fact ε, represents the measure of the quasineutrality degree. The second term in the right-hand side (rhs) of Eq. (33) presents the normalized density of Boltzmannian electrons. The definition of the potential shape we start from the pre-sheath (plasma) equation, when $\varepsilon = 0$ and the quasineutrality condition

$$n_i = \exp[\Phi(x)], \tag{34}$$

is fulfilled. Using (32), Eq. (34) can be presented in the form

$$\begin{aligned} \int_0^{\Phi_s} d\Phi' \frac{dx(\Phi')}{d\Phi'}\exp[(a + \beta - 1)\Phi'] \\ \times \ln\left(\frac{4T_n}{\gamma_E|\Phi' - \Phi|}\right) = C\exp[a\Phi]. \end{aligned} \tag{35}$$

Constants a, C are defined as follows:

$$a = 1 + \frac{1}{2T_n}, \quad C = \frac{1}{\bar{B}} = \sqrt{2\pi T_n}\frac{L}{L_i}, \tag{36}$$

and $\Phi_s = \Phi(x_s)$. After introducing quantity $dx/d\Phi$, in fact, the task consists of deriving the dependence $x = x(\Phi)$ (inverse to the function $\Phi = \Phi(x)$) from integral Eq. (35) of the Fredholm type with the logarithmic kernel.

The solution of the equation of such type, found by Carleman, is given in Ref. 16, pp. 428–429. This solution for our Eq. (35) looks like

This article is copyrighted as indicated in the article. Reuse of AIP content is subject to the terms at: http://scitation.aip.org/termsconditions. Downloaded to IP: 130.183.200.242 On: Tue, 12 Aug 2014 14:08:40

$$\frac{dx_0}{d\Phi} = \frac{C\exp[-(a+\beta-1)\Phi]}{\pi^2\sqrt{\Phi(\Phi_s-\Phi)}} \times \left\{ a\int_{\Phi_s}^{0} dt - \frac{\sqrt{t(\Phi_s-t)}}{t-\Phi}\exp(at) - \frac{\pi}{\ln\left(\frac{16T_n}{\gamma_E|\Phi_s|}\right)}\exp\left(\frac{a\Phi_s}{2}\right) \mathrm{I}_0\left(\frac{a\Phi_s}{2}\right)\right\}, \quad (37)$$

where $\mathrm{I}_0(z)$ $[=\mathrm{I}_0(-z)]$ is the zero order Bessel function of an imaginary argument. The notation $\int$ indicates the principal part of integral. From (37), it follows that the inverse potential profile $x_0 = x_0(\Phi)$ explicitly depends on the ionization factor C,

$$x_0(\Phi) = \frac{2}{\pi^2}C \times \left\{ -a\Phi_s\int_0^1 dq - \sqrt{q(1-q)}e^{+a\Phi_s q} \times \int_0^{\sqrt{\frac{\Phi}{\Phi_s}}} \frac{dz e^{-(a+\beta-1)\Phi_s z^2}}{\sqrt{1-z^2}(q-z)} + \frac{\pi}{\ln\left(\frac{16T_n}{\gamma_E|\Phi_s|}\right)} e^{\frac{a\Phi_s}{2}} \times \mathrm{I}_0\left(\frac{a\Phi_s}{2}\right)\int_0^{\sqrt{\frac{\Phi}{\Phi_s}}} \frac{dz e^{-(a+\beta-1)\Phi_s z^2}}{\sqrt{1-z^2}}\right\}. \quad (38)$$

Following the conventional terminology,[6,7,17] the solution (38), further, we will call "the outer" solution of the two scale analysis. By analogy, the solution describing the actual Debye sheath (see Sec. VI) is called "the inner" solution. The dependence described by Eq. (38) is illustrated in Fig. 2.

The numerical solution for the pre-sheath (plasma) potential profile in the general case, when the kernel of the expansion for the ion density (25) contains the modified Bessel function $\mathrm{K}_0(z)$, is also given in Fig. 2. A comparison of curves in Fig. 2 shows a satisfactory coincidence of the analytic dependence (38) with the numerical ones for high temperatures from the range (30).

The derivative (37) starts with the singularity at $\Phi = 0$ (the minimum of the potential shape) in the center $x = 0$ and becomes zero at the point $x = x_s$, where the expression in the bracket (37) equals to zero. From (37), for the point x_s, we can construct the equation

$$\left\{1 + \frac{2}{a\Phi_s \ln\left(\frac{16T_n}{\gamma_E|\Phi_s|}\right)}\right\} I_0\left(\frac{a\Phi_s}{2}\right) = I_1\left(\frac{a|\Phi_s|}{2}\right), \quad (39)$$

where $I_1(z)$ is the first order Bessel function of an imaginary argument.

The point x_s, where $\Phi = \Phi_s$, corresponds to the electric field singularity and the ultimate breakdown of the quasineutrality approximation expressed by Eq. (34). As usual,[18] the electric field singularity point represents the sheath entrance (or the presheath edge).

The two-scale problem of a plane plasma-wall transition layer, which means $\lambda_D \ll L_s$, implies the plasma or the presheath region (scale L_s) quasineutral, and the sheath (scale λ_D) to be influenced by space charge. In contrast to the more extended presheath, where various effects (in our case ionization) take place, the thin sheath is assumed to be collisionless.

The ions, born at the neutrals' ionization by electron impact, acquire the negative velocity only due to the velocity spreading (also in the negative direction) of the ion source distribution function. In the sheath, where the electron-neutral collisions are absent, an ion cannot be born and consequently in sheath, it means beyond the presheath edge, there are no ions with the negative velocities. This is a reason of the formulation of the condition (b) in Sec. II and choice of Φ_s as upper limit in the integrals in Eqs. (16) and (17).

The dependence of the potential Φ_s at the singular point on the temperature found from Eq. (39) is given in Fig. 3. This dependence is in accordance with the numerical results for $T_n > 1$. After finding Φ_s, we can determine x_s from (38) [see Fig. 4].

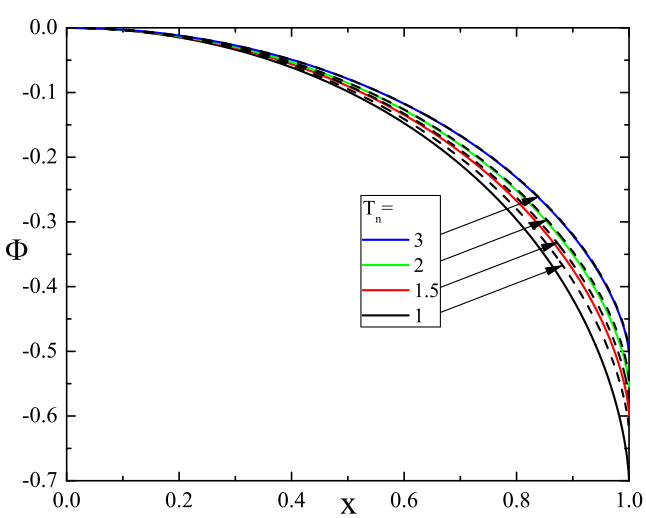

FIG. 2. Calculated potential profiles $\Phi(x_0)$ described by Eq. (38) (solid lines) and numerically obtained potential profiles $\Phi = \Phi(x)$ (dashed lines nearby) scaled to $L_i = 1$ [in the dimensionless units, see Eq. (20)] for $\beta = 1$.

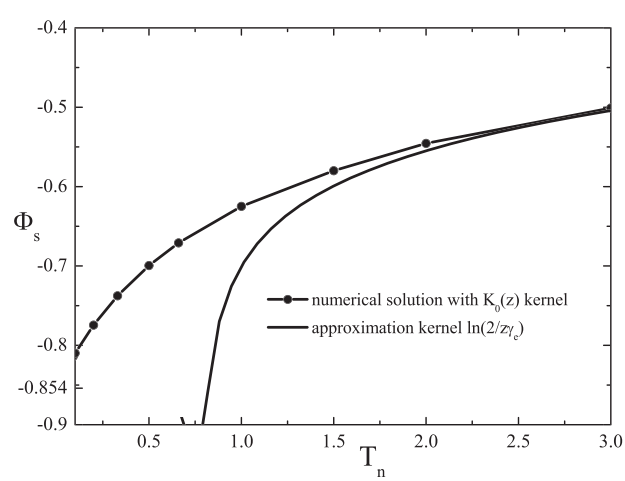

FIG. 3. Sheath edge potential $\Phi_s(T_n)$ from Eq. (39) (solid line) and numerically obtained sheath edge potential (scattered).

This article is copyrighted as indicated in the article. Reuse of AIP content is subject to the terms at: http://scitation.aip.org/termsconditions. Downloaded to IP: 130.183.200.242 On: Tue, 12 Aug 2014 14:08:40

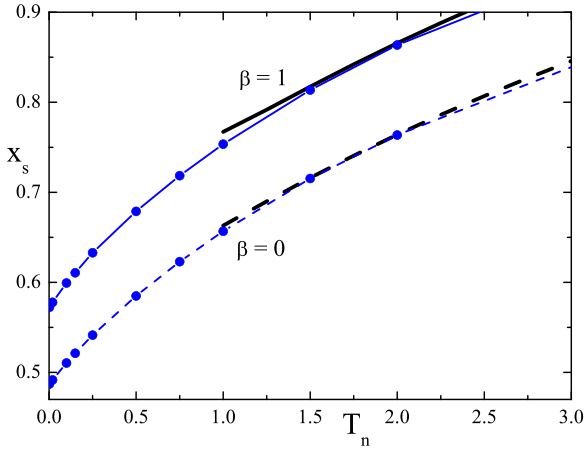

FIG. 4. Dependence of $x_s(T_n)$ for $T_n \geq |\Phi_s|$ (solid for $\beta = 1$ and dashed for $\beta = 0$) in comparison with numerically obtained x_s (blue, scattered).

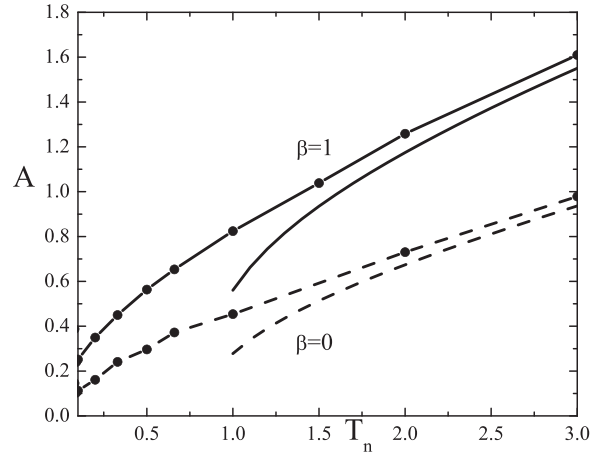

FIG. 5. Coefficient A from Eq. (43) (solid and dashed) and numerically obtained A (scattered) for different β.

As it is mentioned above, the ion source VDF contains in the velocity space the regions with velocities directed in both positive and negative directions. Consequently, newly born ions acquire velocities directed also in opposite directions. Therefore, the averaged ion velocity decreases in comparison with its value obtained if $T_n = 0$ and neutrals are motionless.[7] With increase of the ion source temperature, T_n, the ion average velocity obviously should decrease. This leads to the increase of the ion density and, according to the quasi-neutrality condition (34), to the decrease of the absolute value of the potential $|\Phi|$, $(\Phi < 0)$, including of the pre-sheath edge potential $|\Phi_s|$, simultaneously, the steepness of the potential shape in the Pre-sheath must decrease. Corresponding dependencies of the steepness and on are quite visible.

Using the relation to find the sheath edge potential Φ_s [namely, the equality of the second term in the brackets in the right-hand side of Eq. (37) to the first one at $\Phi = \Phi_s$], we can represent Eq. (37) in the form

$$\frac{dx_{0i}}{d\Phi} = \frac{Ca}{\pi^2}\frac{\exp[-(a+\beta-1)\Phi]}{\sqrt{\Phi(\Phi_s-\Phi)}}(\Phi-\Phi_s) \times \int_{\Phi_s}^{0} dt - \frac{\sqrt{t(\Phi_s-t)}}{(t-\Phi)(t-\Phi_s)}\exp(at). \tag{40}$$

This equation allows to determine the potential profile close to the sheath edge, when $\Phi \simeq \Phi_s$

$$\frac{dx_{oi}}{d\Phi} \simeq -A\sqrt{\Phi-\Phi_s}, \tag{41}$$

or

$$x_{oi} = x_s - \frac{2}{3}A(\Phi-\Phi_s)^{3/2}, \tag{42}$$

where

$$A = \frac{2Ca}{\pi^2}\frac{\exp[-(a+\beta-1)\Phi_s]}{\sqrt{|\Phi_s|}} \times \frac{\partial}{\partial\Phi_s}\int_{\Phi_s}^{0} -dt\frac{\sqrt{|t|(t-\Phi_s)}e^{at}}{(t-\Phi)}\bigg|_{\Phi\to\Phi_s+0} > 0. \tag{43}$$

The dependence of the coefficient A on T_n (or Φ_s) is given in Fig. 5. If coefficient A is transformed with $C_{T_n} = (\frac{2}{3}A)^{-2/3}$ for another definition[10] of the sheath edge singularity, we obtain $C_{T_n}(x_s - x)^{2/3} = \Phi - \Phi_s$.

Obviously, the relations (41) and (42) are valid for $\Phi \geq \Phi_s$ (we remind that $\Phi \leq 0$ and $\Phi_s \leq 0$) and are in accordance with the results of Ref. 10. Quite formally, the relations (41) and (42) can be extended for the region where $\Phi \leq \Phi_s$, assuming

$$\frac{dx_0}{d\Phi} = -A|\Phi-\Phi_s|^{1/2}. \tag{44}$$

According to Refs. 6 and 7 for the smooth connection of the presheath and the sheath solutions, the potential curve near the sheath edge x_s must be symmetric (e.g., for small region from $\Phi > \Phi_s$ and $\Phi < 0$ sides). The expression (44) realizes such a symmetry. The reason for such a extension will be seen from the results given in Secs. VI and VII. So, instead of Eq. (42) we will use

$$x_0 = x_s + \frac{2}{3}A(\Phi_s-\Phi)|\Phi_s-\Phi|^{1/2}. \tag{45}$$

Solutions (42) and (45) can be interpreted as an "inner" expansion of the "outer" solution.[10]

V. BOHM CRITERION

The quasineutral plasma (presheath) ends with the electric field singularity. The corresponding point defines the presheath edge and can not be considered as a wall boundary.

In the frame of the A2S, the presheath should be supplemented by the sheath, where the space charge effect can no longer be neglected. The width of the sheath is of the order of the electron Debye length, and it is assumed to be ionizationless. Therefore, the ion distribution function in the sheath can be found from the homogeneous kinetic equation, that means from Eq. (1) with zero on the right-hand side. Hence, the ion distribution function in the sheath $\bar{f}_s(E)$ can depend only on the total ion energy $E = mv^2/2 + e\Phi$. The explicit

This article is copyrighted as indicated in the article. Reuse of AIP content is subject to the terms at: http://scitation.aip.org/termsconditions. Downloaded to IP: 130.183.200.242 On: Tue, 12 Aug 2014 14:08:40

form of this dependence can be found from the coincidence condition of $\bar{f}_s(E)$ at the sheath edge $x = x_s$ with the ion distribution function (16) in the pre-sheath.

According to considerations given at the end of Sec. IV, in the sheath, there are no ions born there with negative velocities. Hence the sheath ion distribution $\bar{f}_s(\Phi, v)$ can be simply obtained by shifting of $f_i^+(\Phi, v)$ [see Eq. (16)] to the lower potential $\Phi \le \Phi_s$. Introducing the new integration variable $\Phi'' = \Phi' - \Phi_s$, we represent the sheath ion distribution in the form

$$\begin{aligned}\bar{f}_s(v, \Phi) &= \bar{f}_s(v^2 - \chi) \\ &= 2\bar{B}\frac{n_0}{\sqrt{2}c_s}\int_0^{-\Phi_s} d\Phi'' \frac{dx_0(\Phi'')}{d\Phi''}\frac{F_n(\sqrt{2\tau}\sqrt{v^2 - \chi - \Phi''})}{\sqrt{v^2 - \chi - \Phi''}} \\ &\quad \times \exp\left[\beta(\Phi_s + \Phi'')\right]\mathrm{H}(v^2 - \chi - \Phi''). \end{aligned} \tag{46}$$

Here, $\Phi_s < 0$, $\Phi < 0$ and $\chi = \Phi_s - \Phi \ge 0$. It should be mentioned that the necessary sheath edge condition,

$$\bar{f}_s(\Phi_s, v = 0) \;=\; 0, \tag{47}$$

is fulfilled, and also from (46) it follows that $\bar{f}_s(v, \Phi) = 0$ at $v^2 \le \chi$. We remind that for Maxwell distributed ion source F_n in (46) is defined by the relation (19). Further, we use the method given in Ref. 6. For the ion density, considering it as a moment of the "zero order," we have

$$n_i = \frac{1}{2}\int_\chi^\infty y^{-1/2}\bar{f}_s(y - \chi)dy. \tag{48}$$

For the "nth-order" moment, we find

$$M_n = \frac{1}{2}\int_\chi^\infty y^{n-1/2}\bar{f}_s(y - \chi)dy, \tag{49}$$

or

$$M_n = \frac{1}{2}\int_0^\infty dy'(y' + \chi)^{n-1/2}\bar{f}_s(y'). \tag{50}$$

From (4) follows the recurrence relation

$$\begin{aligned}\frac{dM_n}{d\Phi} &= -\left(n - \frac{1}{2}\right)\frac{1}{2}\int_0^\infty dy'(y' + \chi)^{n-1-1/2}\bar{f}_s(y') \\ &= -\left(n - \frac{1}{2}\right)M_{n-1}. \end{aligned} \tag{51}$$

At the sheath edge, $n_{is} = \exp(\Phi_s)$ and consequently $M_{0s} = n_s = \exp(\Phi_s)$. Then according to (51),

$$M_{-1s} = 2\,n_s. \tag{52}$$

Finally, from (49), we find

$$\frac{1}{2n_s}\int_0^\infty \frac{dy}{y^{3/2}}\bar{f}_s(y) = \left\langle \frac{1}{v^2}\right\rangle_s = 2. \tag{53}$$

It means that the kinetic Bohm criterion is fulfilled in the marginal form also in the case of hot neutrals. In the integral (53) does not arise a mathematical difficulty due to divergence if the integrand at the point $y \equiv v^2 = 0$, as at this point the distribution function vanishes [see Eq. (47)].

VI. ANALYSIS OF AN ASYMPTOTIC SHEATH

Using the sheath scale ($\simeq \lambda_D$) and introducing corresponding coordinates Poisson's equation, we can write in the form

$$\frac{d^2\chi}{d\xi^2} = n_i - n_e, \tag{54}$$

where

$$\xi = (x - x_r)/\varepsilon \quad \text{and} \quad \chi = \Phi_s - \Phi. \tag{55}$$

x_r is an arbitrary reference point allowing a suitable choice of origin for the sheath coordinate ξ. Further, we will again follow the procedure given in Ref. 6. Relating the potential to the sheath edge from (48) for the ion and electron densities, we find

$$n_i(\chi) = \frac{1}{2}\int_0^\infty \frac{dy}{\sqrt{\chi + y}}\bar{f}_s(y), \tag{56}$$

$$n_e(\chi) = \exp(\Phi_s - \chi). \tag{57}$$

Further, we will use the following boundary condition: $d\chi/d\xi \to 0$ at $\chi \to 0$. After integration from (54), we obtain

$$\frac{d\chi}{d\xi} = \left\{2\int_0^\infty dy\bar{f}_s(y)\left[\sqrt{\chi + y} - \sqrt{y}\right] + 2e^{\Phi_s}[e^{-\chi} - 1]\right\}^{1/2}. \tag{58}$$

We give Eq. (58) in the form that is more convenient for numerical calculations

$$\xi - \xi_w = \int_{\chi_w}^{\chi} \frac{d\psi}{\left\{2[W(\psi) + \exp(\Phi_s - \psi) - \exp(\Phi_s)]\right\}^{1/2}}, \tag{59}$$

where ξ_w and χ_w are the wall coordinate and the relative potential at the wall, and

$$W(\psi) = \int_0^\infty dy\bar{f}_s(y)[\sqrt{\psi + y} - \sqrt{y}]. \tag{60}$$

The smallness of the relative potential in the vicinity of the sheath edge $\chi \ll 1$ allows us to find the analytic expression for the potential shape there.;in other words, to find the "outer" expansion of "inner" (sheath) solution (59). Obviously, the numerical solution of Eq. (59) must coincide with this analytic expression in the indicated region. We start with expansion of the ion and electron densities

$$n_i(\chi) = \sum_{\nu=0}^{\infty} a_\nu \chi^{\nu/2}, \tag{61}$$

$$n_e(\chi) = \exp(\Phi_s)\sum_{\nu=0}^{\infty} b_\nu \chi^\nu, \tag{62}$$

This article is copyrighted as indicated in the article. Reuse of AIP content is subject to the terms at: http://scitation.aip.org/termsconditions. Downloaded to IP: 130.183.200.242 On: Tue, 12 Aug 2014 14:08:40

where

$$a_{2n} = \frac{(-1)^n}{2n!}\int_0^\infty \frac{dy}{\sqrt{y}}\frac{d^n\bar{f}_s(y)}{dy^n}, \tag{63}$$

$$a_{2n+1} = \frac{\pi(-1)^{n+1}}{2(n+\frac{1}{2})!}\frac{d^n\bar{f}_s(y)}{dy^n}\bigg|_{y=0}, \tag{64}$$

$$b_n = \frac{(-1)^n}{n!}. \tag{65}$$

(The detailed calculations to obtain Eqs. (63) and (64) one can find in Refs. 6 and 18.) For the Poisson equation (54), we then have

$$\frac{d^2\chi}{d\xi^2} = \sum_\nu c_\nu \chi^{\nu/2}, \tag{66}$$

where

$$c_\nu = \begin{cases} a_{2n} - b_n \exp(\Phi_s) & \text{for } \nu = 2n, \\ a_{2n+1} & \text{for } \nu = 2n+1. \end{cases} \tag{67}$$

For coefficients c_ν, we have

1. according to the quasineutrality condition at the sheath edge

$$c_0 = \frac{1}{2}\int_0^\infty \frac{dy}{\sqrt{y}}\bar{f}_s(y) - \exp(\Phi_s) = 0, \tag{68}$$

2. due to boundary condition (47) for the distribution function at the sheath edge

$$c_1 = -\frac{1}{\sqrt{\pi}}\,\bar{f}_s(0) = 0, \tag{69}$$

3. and the Bohm criterion, presented in the form (52), gives $c_2 = 0$.

Therefore, apparently the first non-vanishing coefficient in the series (66) is

$$c_3 = \frac{2}{3}\frac{d\bar{f}_s(y)}{dy}\bigg|_{y=0}. \tag{70}$$

Neglecting higher order terms from (66), we find

$$\xi_{io} = \xi_0 - 2\sqrt{\frac{5}{c_3}}\frac{1}{\chi^{1/4}}. \tag{71}$$

The integration constant ξ_0 and its relation to the ξ_w should be found by comparison of Eq. (71) with numerical solution of Eq. (59) [see Fig. 6]. It follows that a potential drop in sheath for hydrogen at $T_{n1} = 0.5$, $\chi_w = \Phi_s(T_{n1}) - \Phi_w(T_{n1}) = 2.676$ and at $T_{n2} = 1.0$ $\chi_w = \Phi_s(T_{n2}) - \Phi_w(T_{n2}) = 2.634$ [here $\Phi_w(T_n)$ is the wall floating potential; see Fig. 6]. The comparison of the numerical solution of Eq. (59) for small χ with Eq. (71) gives

$$\begin{aligned} \xi_0 &= \xi_w + 3.81 \quad \text{at} \quad T_n = 0.1, \\ \xi_0 &= \xi_w + 3.72 \quad \text{at} \quad T_n = 0.5, \\ \xi_0 &= \xi_w + 3.52 \quad \text{at} \quad T_n = 1, \ \text{and} \\ \xi_0 &= \xi_w + 3.28 \quad \text{at} \quad T_n = 2. \end{aligned} \tag{72}$$

VII. INTERMEDIATE REGION AND ITS SCALE

The asymptotic presheath and sheath regions are the result of considering the limit $\varepsilon = (\lambda_L/L_i) \to 0$, The presheath is assumed to be quasineutral, which leads to the electric field singularity at the presheath edge, while in the sheath, the space change has a crucial importance, and the ionization is neglected. Obviously, in order to connect these two regions, one has to introduce some intermediate region, which will take into account both effects—the space change and ionization at least in the first non-vanishing approximation. Using the expression for the ion density (25), we represent Poisson's equation in the following form:

$$-\varepsilon^2\frac{d^2\Phi}{dx^2} = \bar{B}\int_0^{\Phi_s} d\Phi' \frac{dx(\Phi')}{d\Phi'}\exp[(a+\beta-1)\Phi'] \times \mathrm{K}_0\left(\frac{|\Phi'-\Phi|}{2T_n}\right)\exp[-(a-1)\Phi] - \exp(\Phi). \tag{73}$$

At $\varepsilon = 0$, Eq. (73) results in Eq. (35) for the presheath at the high temperature (30), with the dependence $x_0 = x_0(\Phi)$ defined by (38).

The results obtained below are valid for the temperatures (30), but, for convenience, we will operate further with the Bessel function $\mathrm{K}_0(z)$ instead of its logarithmic approximation. Expressing $\exp(\Phi)$ from the plasma (presheath) approximation, we obtain

$$-\varepsilon^2\frac{d^2\Phi}{dx^2} = \bar{B}\int_0^{\Phi_s} d\Phi' \exp(\beta\Phi')\exp[(a-1)(\Phi'-\Phi)] \times \mathrm{K}_0\left(\frac{|\Phi'-\Phi|}{2T_n}\right)\frac{d}{d\Phi'}\{x(\Phi') - x_0(\Phi')\}, \tag{74}$$

where $x_0(\Phi)$ is defined by Eq. (38).

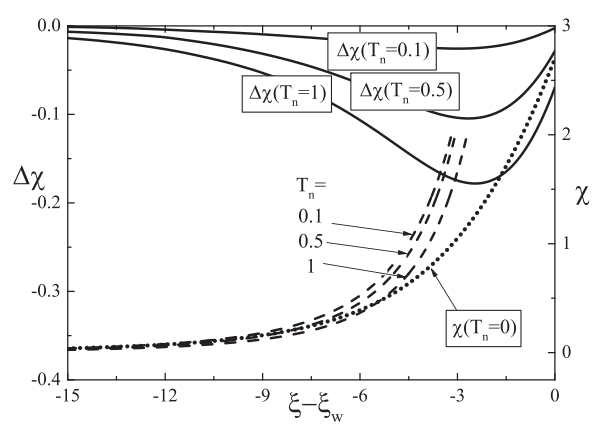

FIG. 6. Potential deviation $\Delta\chi = \chi_{T_n} - \chi_0$ from its value χ_0 at $T_n = 0$ in hydrogen plasma for $T_n = 0.1$, 0.5, 1 for $\beta = 1$. The dotted line shows the shape of $\chi_0(\xi - \xi_w)$ [cf. Ref. 6, Fig. 3]. The dashed lines correspond to the plasma sided expansion $\xi_{io}(\chi)$ from Eq. (71). On the ordinate axis (in the right-hand side) are given values $\chi_w = \Phi_s - \Phi_w$ with the wall floating potentials Φ_w for hydrogen.

This article is copyrighted as indicated in the article. Reuse of AIP content is subject to the terms at: http://scitation.aip.org/termsconditions. Downloaded to IP: 130.183.200.242 On: Tue, 12 Aug 2014 14:08:40

We are interested in the asymptotic limit $\varepsilon \to 0$, $(\varepsilon \neq 0)$ and restrict ourselves by analysis of a small region near the sheath edge $\Phi = \Phi_s$. The difference between $x(\Phi)$ and $x_0(\Phi)$ may be neglected in the plasma (presheath) region, whence it follows that $x(0) = x_0(0)$. Therefore, in fact, the integration interval in Eq. (74) is narrowed to the small interval adjoining to the upper limit Φ_s,[4,6] so we can

(i) replace Φ and Φ' with Φ_s in exponential functions.
(ii) approximate $x_0(\Phi)$ with the solution (42).
After partial integration from Eq. (74), we obtain

$$-\varepsilon^2 \frac{d^2\Phi}{dx^2} = \bar{B} e^{\beta\Phi_s} \left\{ \mathrm{K}_0\left(\frac{|\Phi - \Phi_s|}{2T_n}\right)[x(\Phi_s) - x_0(\Phi_s)] - \mathrm{K}_0\left(\frac{|\Phi|}{2T_n}\right)[x(0) - x_0(0)] - \int_0^{\Phi_s} d\Phi' \left[\frac{\partial}{\partial\Phi'}\mathrm{K}_0\left(\frac{|\Phi' - \Phi|}{2T_n}\right)\right] \cdot [x(\Phi') - x_0(\Phi')] \right\}. \tag{75}$$

The second term in the right-hand side of Eq. (75) is equal to zero. Please note that the derivative $\partial/\partial\Phi' \mathrm{K}_0\,[|\Phi' - \Phi|/(2T_n)] = -\mathrm{K}_1(|\Phi' - \Phi|/(2T_n))$ and that both Bessel functions $\mathrm{K}_0(z)$ and $\mathrm{K}_1(z)$ decrease fast at the increasing of their arguments.[19] Therefore, at a non-zero neutral temperature, $T_n \neq 0$, we can assume that the region $\Phi' \simeq \Phi$ gives the main contribution in the integral (76) and write

$$-\varepsilon^2 \frac{d^2\Phi}{dx^2} = \bar{B} \exp(\beta\Phi_s) \left\{ \mathrm{K}_0\left(\frac{|\Phi - \Phi_s|}{2T_n}\right)[x(\Phi_s) - x_0(\Phi_s)] - \int_0^{\Phi_s} d\Phi' \left[\frac{\partial}{\partial\Phi'}\mathrm{K}_0\left(\frac{|\Phi' - \Phi|}{2T_n}\right)\right] \cdot [x(\Phi) - x_0(\Phi)] \right\}. \tag{76}$$

After integration, we find

$$-\varepsilon^2 \frac{d^2\Phi}{dx^2} = \bar{B} \exp(\beta\Phi_s) \left\{ \mathrm{K}_0\left(\frac{|\Phi - \Phi_s|}{2T_n}\right) \times [(x(\Phi_s) - x_0(\Phi_s)) - (x(\Phi) - x_0(\Phi))] + K_0\left(\frac{|\Phi|}{2T_n}\right)[x(\Phi) - x_0(\Phi)] \right\}. \tag{77}$$

The first term in the right-hand side of Eq. (77) is of order $(\Phi - \Phi_s)$, and we can neglect it as

$$\mathrm{K}_0\left(\frac{|\Phi - \Phi_s|}{2T_n}\right)(\Phi - \Phi_s) \to 0 \quad \text{at} \quad (\Phi - \Phi_s) \to 0. \tag{78}$$

Finally, we obtain

$$-\varepsilon^2 \frac{d^2\Phi}{dx^2} = \bar{B} e^{\beta\Phi_s} \mathrm{K}_0\left(\frac{|\Phi_s|}{2T_n}\right)[x(\Phi) - x_0(\Phi)]. \tag{79}$$

Introducing the intermediate scale variables ζ and ζ_0 by

$$x = x_s + \frac{2}{3}A\delta^{3/2}\zeta, \qquad x_0 = x_s + \frac{2}{3}A\delta^{3/2}\zeta_0, \tag{80}$$

and restricting ourselves by analysis of the sheath edge vicinity

$$\Phi = \Phi_s - \delta \cdot w \qquad (\delta \ll 1), \tag{81}$$

we obtain from Eq. (79)

$$\frac{d^2 w}{d\zeta^2} = \bar{B} \exp(\beta\Phi_s)\mathrm{K}_0\left(\frac{|\Phi_s|}{2T_n}\right)\frac{8}{27}A^3\frac{\delta^{7/2}}{\varepsilon^2}(\zeta - \zeta_0). \tag{82}$$

Choosing

$$\delta = \left\{ \frac{27}{8}\frac{\exp(-\beta\Phi_s)}{\bar{B}A^3\mathrm{K}_0\left(\frac{|\Phi_s|}{2T_n}\right)} \right\}^{2/7} \varepsilon^{4/7}, \tag{83}$$

and taking into account, that

$$\zeta_0 = \frac{x_0 - x_s}{\frac{2}{3}A\delta^{3/2}} = -|\mathrm{w}|^{3/2}, \tag{84}$$

we give to Poisson's equation the form

$$\frac{d^2 w}{d\zeta^2} = \zeta + |\mathrm{w}|^{3/2}, \tag{85}$$

which describes the intermediate region of the Tonks–Langmuir model with the ion source having the temperatures (30). By means of Eq. (83), for the intermediate scale length, we find

$$\ell = \left\{ \frac{9}{4}\frac{\exp(-3\beta\Phi_s)}{\bar{B}^3A^2\mathrm{K}_0^3\left(\frac{|\Phi_s|}{2T_n}\right)} \right\}^{1/7} \lambda_D^{6/7}L_s^{1/7}. \tag{86}$$

From the transformations (81) and (83) and from the estimation $dw/d\zeta = O(1)$, we can conclude that the intermediate region is distinguished by the electric field

$$E \sim \frac{kT_e}{e}\left\{\frac{\bar{B}\mathrm{K}_0[|\Phi_s|/(2T_n)]}{A^4\exp(-\beta\Phi_s)}\right\}^{1/7} \cdot \frac{1}{\lambda_D^{2/7}L_s^{5/7}}. \tag{87}$$

For the case when $T_n = 0$, we can use the results of Refs. 4 and 6, where for the scale-length and the characteristic electric field in the intermediate region the following expressions are given, respectively:

$$l_m \sim \frac{1}{a^{1/3}}\left\{\frac{3\sqrt{3}}{8}\exp(-\Phi_s)\right\}^{1/9} \cdot \lambda_D^{8/9}L_s^{1/9}, \quad a \cong 0.335, \tag{88}$$

$$E \sim \frac{kT_e}{e}\frac{1}{a^{1/3}}\left\{\frac{8}{3\sqrt{2}}\exp(\Phi_s)\right\}^{2/9} \cdot \frac{1}{\lambda_D^{4/9}L_s^{5/9}}. \tag{89}$$

In obtaining (88) and (89), we have used the relation for the ionization length, found in Ref. 13. At comparison of (86) with (88) and (87) with (89), the essential change of dependences of the intermediate scale-length and the electric field on the characteristic parameters Φ_s, λ_D and L_s for $T_n \neq 0$ is obvious.

This article is copyrighted as indicated in the article. Reuse of AIP content is subject to the terms at: http://scitation.aip.org/termsconditions. Downloaded to IP: 130.183.200.242 On: Tue, 12 Aug 2014 14:08:40

Neglecting in Eq. (85) the left-hand side (the space charge term), we obtain the presheath approximation solution (41). Keeping the space charge term and neglecting the collisional (ionization) contribution, represented in Eq. (85) by the first term in the right-hand side, we obtain the sheath approximation described in Sec. VI. Consequently, as a solution of the equation

$$\frac{d^2w}{d\zeta^2} = w^{3/2}, \quad w > 0, \tag{90}$$

we find

$$\zeta = \overline{\zeta_0} - \sqrt{20}\; w^{-1/4}. \tag{91}$$

Hence, at $\zeta \to \overline{\zeta_0}$, we have a singularity $w \to \infty$. The numerical calculations for this singular point gives $\overline{\zeta_0} = 5.1545576$. The location of this singularity is crucial for the indication of the sheath and wall's location (see Sec. IX). A comparison of Eqs. (71) and (91) and definitions of the sheath (55) and intermediate (80) coordinates shows that Eq. (91) correctly describes the "outer" expansion of the "inner" solution (71). For the coefficient c_3, we find

$$c_3 = \frac{9}{4}\frac{\varepsilon^2}{A^2\delta^{7/2}}. \tag{92}$$

The numerical calculations show the correctness of this relation. Hence, Eq. (85) should realize a smooth transition between the "outer" (presheath) and the "inner" (sheath) solutions.

In Fig. 7 are presented $w(\zeta)$ and its asymptotics corresponding to the "outer" and "inner" expansions. Equation (90) and its solution (91) are in accordance with Eq. (45) and justify the extensions made in the end of Sec. IV (see remarks there).

VIII. MATCHING OF SOLUTIONS

According to the results found in Secs. IV–VII, we know the three different asymptotic solutions: $\Phi = \Phi(x_0)$ for the presheath from Eq. (38), $w(\zeta)$ for the intermediate region from Eq. (85), and $\chi(\xi)$ for the Debye sheath from Eq. (59). For small but finite ε, these solutions can be bridged and one can in the satisfactory form construct a potential shape describing the PWT layer as a whole. Obviously, this procedure can be realized at the existence of a range of common validity of the different solutions mentioned above. Below we will perform two following matching procedures that are graphed in Fig. 8.

A. Matching of the plasma (presheath) and the intermediate solutions

The "inner" expansion of the "outer" (presheath) solution [see Eq. (42)] must have the same form as the "outer" expansion $\zeta_{oi}(w)$ of the intermediate solution [see Eq. (84)]. Keeping in mind Eqs. (42), (80), and (84), we find

$$\begin{aligned} x_{oi} &= x_s - \frac{2}{3}A\delta^{3/2}\zeta_0, \\ \zeta_0 &= \delta^{-3/2}(\Phi - \Phi_s)^{3/2}, \end{aligned} \tag{93}$$

and hence, the matching solution is fulfilled by construction. It confirms the range of common validity of the plasma and intermediate solutions. Introducing the inverse to $x_0(\Phi)$, $\zeta(w)$ and $x_{oi}(\Phi)$ functions [$\Phi(x)$, $\Phi_{mo}(x,\varepsilon)$, and $\Phi_{oi}(x,\varepsilon)$, respectively] according to the usual rule of the asymptotic analysis,[17] we can construct the following matched asymptotic expression:

$$\Phi_1(x,\varepsilon) = \Phi_0(x) + \Phi_{mo}(x,\varepsilon) - \Phi_{oi}(x,\varepsilon). \tag{94}$$

For small $\varepsilon \neq 0$, this expression should describe the reasonable approximation for the smooth transition from the presheath to the intermediate region.

B. Matching of the intermediate and the sheath solutions

Obviously, for the realization of the matching, the "inner" expansion of the intermediate solution (91) must be

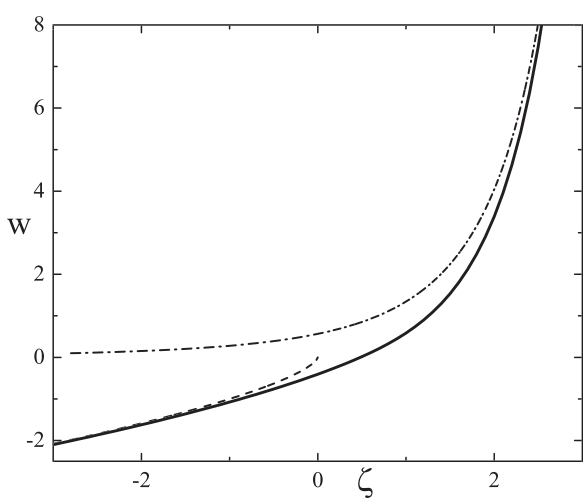

FIG. 7. Intermediate solution $w(\zeta)$, its sheath $(- \cdot - \cdot - \cdot -)$ and presheath (plasma) $(- - - -)$ approximations.

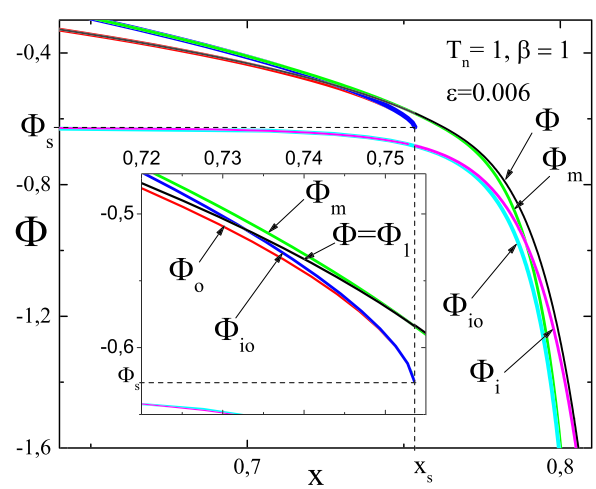

FIG. 8. Detail of the matched approximation nearby the point (Φ_s, x_s). Inset graph shows zoomed presheath solution Φ_1 with x_s aligned.

This article is copyrighted as indicated in the article. Reuse of AIP content is subject to the terms at: http://scitation.aip.org/termsconditions. Downloaded to IP: 130.183.200.242 On: Tue, 12 Aug 2014 14:08:40

in accordance with the "outer" expansion (71) of the "inner" (sheath) solution. From (80) and (55), we have

$$x_s + \frac{2}{3}A\delta^{3/2}\zeta = x_r + \varepsilon\xi. \tag{95}$$

To insure this relation, we have to use the solutions (91) and (71). Equalizing the coefficients in front of $\chi^{-1/4}$, we have already found the constant c_3 [see (92)]. The equality of the free (from χ) terms in (95) connects the integration constant ξ_0 with intermediate singular point $\overline{\zeta_0}$:

$$\xi_0 = \frac{x_s - x_r + \frac{2}{3}A\delta^{3/2}\overline{\zeta_0}}{\varepsilon}. \tag{96}$$

Such a choice of ξ_0 ensures validity of the matching condition and adjusts the position of the sheath to the intermediate region.[6,7] The relation (96) also allows to define the reference point x_r in the most convenient way, assuming $x_r = x_s$, supposing the sheath edge as only universal point in analysis of the intermediate and the sheath regions.[7] From (96) then we have

$$\xi_0 = \frac{2}{3}\frac{1}{\varepsilon}A\delta^{3/2}\overline{\zeta_0}. \tag{97}$$

Inverse to relations (59), (71), and (91) expressions define the following functions, respectively: $\Phi_i(x,\varepsilon)$: the asymptotic sheath potential (the "inner" solution); $\Phi_{io}(x,\varepsilon)$: the "outer" expansion of the "inner" solutions; and $\Phi_{mi}(x,\varepsilon)$: the "inner" expansion of the intermediate solution.

By means of these functions, we can represent the matching in the following analytic form:

$$\Phi_2(x) = \Phi_{mi}(x,\varepsilon) - \Phi_{io}(x,\varepsilon) + \Phi_i(x,\varepsilon). \tag{98}$$

C. Unified matching of the presheath and the sheath

Equations (94) and (98), obtained at the approximations mentioned above, are valid in the plasma (presheath) and the intermediate regions, and in the intermediate and the sheath regions, respectively. From these equations, it follows that outside of the intermediate region the potential shape $\Phi(x)$ in the plasma region $x \le x_s$ is defined by $\Phi_o(x)$, $\Phi(x) \simeq \Phi_o(x)$, and $\Phi(x) \simeq \Phi_i(x,\varepsilon)$ for $x > x_s$. This allows to combine (94) and (98) in the unified matched expression

$$\bar{\Phi}(x) = \Phi_o(x) - \Phi_{oi}(x,\varepsilon) + \Phi_m(x,\varepsilon) - \Phi_{io}(x,\varepsilon) + \Phi_i(x,\varepsilon), \tag{99}$$

where $\Phi_m(x,\varepsilon)$ is the potential in the intermediate region satisfying Eq. (85). The validity of the approximation (99) is restricted by the extremely low values of ε, as it is shown in Fig. 9. In Fig. 10 is given dependence of the ion density n_i on the potential Φ for various T_n found by means of Eq. (18).

IX. THE EIGENVALUE PROBLEM

In the method used here, to describe the Tonks–Langmuir model, the wall localization x_w is not *a priori* given. It is an eigenvalue of a problem arising due to the requirement of the "plasma balance:" the necessary adjustment of the ion production rate in the ionization process to the ion loss at the wall. This eigenvalue should be found by cutting the potential curve at that point $x = x_w$, where the wall boundary condition $\Phi(x_w) = \Phi_w$ is fulfilled:

$$x_w = \lambda(\Phi_w, \varepsilon). \tag{100}$$

For the wall potential, we choose the floating potential in the hydrogen plasma, $\Phi_w(T_n = 0.1) = -3.511$, $\Phi_w(T_n = 1) = -3.259$. At $\varepsilon \to 0$, the wall's position equals to the sheath edge

$$\lambda_0 = x_s. \tag{101}$$

Constructing the next approximation for the finite (but small) ε, we have to take into account the contribution of the intermediate region. Obviously, this contribution should be terminated by the singularity at $\overline{\zeta_0}$

$$\lambda_1 = x_s + \frac{2}{3}A\delta^{3/2}\overline{\zeta_0}. \tag{102}$$

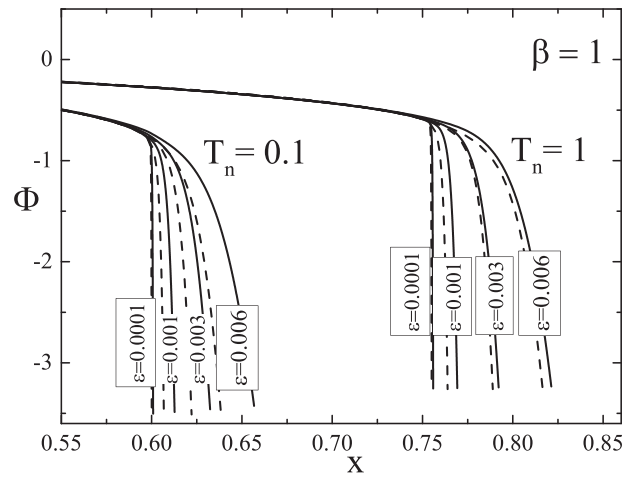

FIG. 9. Comparison of the matched approximation: $\bar{\Phi}(x)$ according to Eq. (99) (—) and the exact numerical potential $\Phi(x)$ (– –) according to Eq. (33) for various values of T_n and ε. The wall potential Φ_w equals to the floating potential in hydrogen.

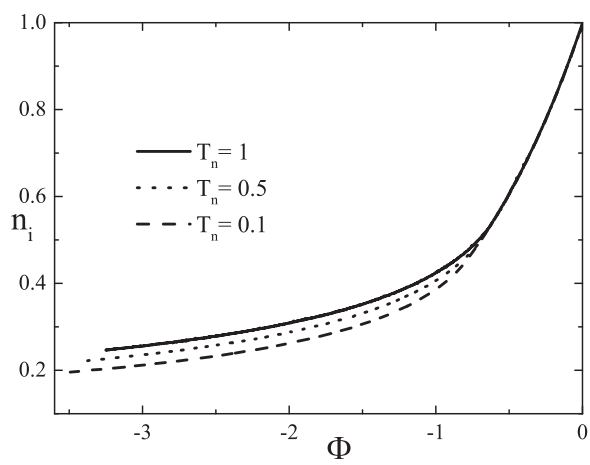

FIG. 10. Dependencies of the n_i on the Φ for different T_n at $\beta = 1$. The wall potential is equal to the floating potential in the hydrogen gas.

This article is copyrighted as indicated in the article. Reuse of AIP content is subject to the terms at: http://scitation.aip.org/termsconditions. Downloaded to IP: 130.183.200.242 On: Tue, 12 Aug 2014 14:08:40

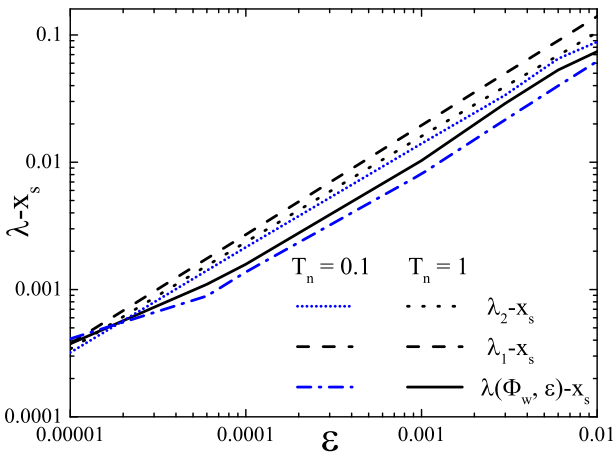

FIG. 11. Dependence of the differences $\lambda(\Phi_w, \varepsilon) - x_s$ [$\lambda(\Phi_w, \varepsilon)$ is the eigenvalue found from the complete Eq. (33)], and its approximations $\lambda_1 - x_s$ [see Eq. (102)] and $\lambda_2 - x_s$ [see Eq. (103)] on ε and T_n for $\Phi_w(T_n = 0.1) = -3.511$, $\Phi_w(T_n = 1) = -3.259$ and $\beta = 1$. The curves for $\lambda_1 - x_s$ coincide at $T_n = 0.1$ and $T_n = 1$.

The contribution of the sheath becomes appreciable only in the next order approximation

$$\lambda_2 = x_s + \frac{2}{3} A \delta^{3/2} \overline{\zeta_0} + \varepsilon(\xi_w - \xi_0). \tag{103}$$

According to Eq. (72), the sheath contribution in (103) is negative, as it was expected. Dependencies of the exact eigenvalue λ and its approximate values λ_1 and λ_2 on ε and T_n are plotted in Fig. 11. The curves show that approximation λ_2 is quite contented for small values of ε.

X. SUMMARY

In this paper, we have provided the kinetic analysis of the classical T&L model of the electric discharges, where plasma is assumed to be weakly ionized and ions' creation takes place due to neutral particles ionization by the electron impact. To our knowledge, this is a first attempt for the comprehensive kinetic investigation of the whole [including the pre-sheath PS) and DS] T&L model taking into account thermal motion of ion source particles. Using the A2S approximation, the presheath and the Debye sheath are studied separately from each other, which allows to follow the "beaten track" of the PWT investigation starting our derivation from the PS and proceedings to the position where the wall boundary condition, $\Phi = \Phi_w$, is fulfilled. The comparison of exact numerical results (see Fig. 11) with the PS and DS matching procedure shows that the A2S approximation correctly describes the PWT layer.

The definition of the wall position is directly connected with solution of the "eigenvalue problem." Physically, this problem reflects the fact that the ion production rate must be equal to the rate of ion loss onto wall. The intermediate scale analysis is performed to describe PS–DS transition and to enable smooth matching of these neighboring sublayers. The equation which describes the intermediate region and bridges the PS and the DS is derived. The intermediate scale length is found.

The results can more adequately describe the physical situation at the solid walls in the laboratory plasmas and the divertor plates in tokamak.

ACKNOWLEDGMENTS

This work was supported by the European Commission under (i) the Contract of Association between EURATOM and the Austrian Academy of Sciences and by (ii) the Austrian Science Fund (FWF) under Project Nos. P22345-N16 and P19333-N16. It was carried out within the framework of the European Fusion Development Agreement. The views and opinions expressed herein do not necessarily reflect those of the European Commission. The authors are indebted to K.-U. Riemann for helpful discussions. We are also grateful to Professor J. Duhovnik and Professor S. Kuhn for their support in various aspects of our investigations.

[1]L. Tonks and I. Langmuir, Phys. Rev. **34**, 876 (1929).
[2]A. Caruso and A. Cavaliere, Nuovo Cimento (1955–1965) **26**, 1389 (1962).
[3]E. R. Harrison and W. B. Thompson, Proc. Phys. Soc. **74**, 145 (1959).
[4]K.-U. Riemann, J. Phys. D: Appl. Phys. **36**, 2811 (2003).
[5]D. Bohm, in *The Characteristics of Electrical Discharges in Magnetic Fields*, 1st ed., edited by A. Guthrie and R. K. Wakerling (McGraw-Hill, New York, 1949), Chap. 2.5, pp. 49–86.
[6]K.-U. Riemann, Phys. Plasmas **13**, 063508 (2006).
[7]K.-U. Riemann, J. Seebacher, D. D. Tskhakaya, Sr., and S. Kuhn, Plasma Phys. Controlled Fusion **47**, 1949 (2005).
[8]R. C. Bissell and P. C. Johnson, Phys. Fluids **30**, 779 (1987).
[9]J. T. Scheuer and G. A. Emmert, Phys. Fluids **31**, 3645 (1988).
[10]L. Kos, D. D. Tskhakaya, and N. Jelić, Phys. Plasmas **18**, 053507 (2011).
[11]A. Emmert, R. M. Wieland, A. T. Mense, and J. N. Davidson, Phys. Fluids **23**, 803 (1980).
[12]L. Kos, N. Jelić, S. Kuhn, and J. Duhovnik, Phys. Plasmas **16**, 093503 (2009).
[13]N. Jelić, L. Kos, D. D. Tskhakaya, Sr., and J. Duhovnik, Phys. Plasmas **16**, 123503 (2009).
[14]K.-U. Riemann, private communication (2009).
[15]S. Gradstein and I. M. Ryshik, *Summen-, Produkt- und Integral-Tafeln*, 1st ed. (Verlag Harri Deutsch, Thun, 1981).
[16]G. F. Carrier, M. Krook, and C. E. Pearson, *Functions of a Complex Variable: Theory and Technique* (Mcgraw-Hill, New York, 1966).
[17]M. van Dyke, *Perturbation Methods in Fluid Mechanics* (Academic Press, New York, 1964), p. 84.
[18]K.-U. Riemann, J. Phys. D: Appl. Phys. **24**, 493 (1991).
[19]M. Abramovitz and I. A. Stegun, *Handbook of Mathematical Functions with Formulas, Graphs and Mathematical Tables* (Dover, New York, 1974).

This article is copyrighted as indicated in the article. Reuse of AIP content is subject to the terms at: http://scitation.aip.org/termsconditions. Downloaded to IP: 130.183.200.242 On: Tue, 12 Aug 2014 14:08:40